

# Key Emerging Issues and Recent Progress related to Structural Materials Degradation

*Author*

Francois Cattant  
Plescop, France



A.N.T. INTERNATIONAL®

© December 2018

Advanced Nuclear Technology International  
Spinnerivägen 1, Mellersta Fabriken plan 4,  
448 50 Tollerød, Sweden

[info@antinternational.com](mailto:info@antinternational.com)

[www.antinternational.com](http://www.antinternational.com)

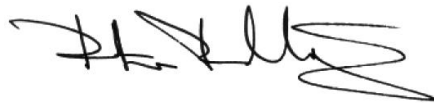


Ecolabelled printed matter, 4041 0799

## **Disclaimer**

The information presented in this report has been compiled and analysed by Advanced Nuclear Technology International Europe AB (ANT International®) and its subcontractors. ANT International has exercised due diligence in this work, but does not warrant the accuracy or completeness of the information. ANT International does not assume any responsibility for any consequences as a result of the use of the information for any party, except a warranty for reasonable technical skill, which is limited to the amount paid for this report.

**Quality-checked and authorized by:**

A handwritten signature in black ink, appearing to read 'Peter Rudling', with a stylized flourish at the end.

Mr Peter Rudling, President of ANT International

## Contents

<b>1</b>	<b>Introduction</b>	<b>1-1</b>
1.1	General information	1-1
1.2	Summary	1-2
<b>2</b>	<b>Papers summaries</b>	<b>2-1</b>
2.1	PWR Nickel SCC – SCC	2-1
2.2	PWR Nickel SCC – Initiation	2-11
2.3	PWR Nickel SCC—Aging Effects	2-20
2.4	PWR Nickel SCC—Alloy 600 Mechanistic	2-34
2.5	PWR Nickel SCC—Alloy 690 Mechanistic	2-48
2.6	Irradiation Damage—Stainless Steel	2-60
2.7	Irradiation Damage—Swelling	2-68
2.8	Irradiation Damage—Nickel Based and Low Alloy	2-74
2.9	PWR Stainless Steel SCC and Fatigue – SCC	2-77
2.10	PWR Stainless Steel SCC and Fatigue—Fatigue	2-95
2.11	Special Topics	2-105
2.12	Accident Tolerant Fuel Cladding	2-113
2.13	BWR SCC and Water Chemistry	2-116
2.14	Stainless Steel Aging and CASS	2-136
2.15	Welds, Weld Metals, and Weld Assessments	2-144
2.16	Plant Operating Experience	2-153
2.17	IASCC Testing—Characterization	2-171
2.18	PWR Secondary Side	2-178

References

Nomenclature

List of Abbreviations

Unit conversion

# 1 Introduction

## 1.1 General information

This document is an extensive summary of the 18<sup>th</sup> International Conference on Environmental Degradation of Materials in Nuclear Power Systems – Water Reactors held August 13-17, 2017 in Portland, Oregon, USA.

The conference had 25 tracks and a poster session. The 25 tracks are listed hereafter:

- PWR Nickel SCC—SCC
- PWR Nickel SCC—Initiation
- PWR Nickel SCC—Aging Effects
- PWR Nickel SCC—Alloy 600 Mechanistic
- PWR Nickel SCC—Alloy 690 Mechanistic
- Irradiation Damage—Stainless Steel
- Irradiation Damage—Swelling
- Irradiation Damage—Nickel Based and Low Alloy
- PWR Stainless Steel SCC and Fatigue—SCC
- PWR Stainless Steel SCC and Fatigue—Fatigue
- Special Topics I—Materials
- Special Topics II—Processes
- Cables and Concrete Aging and Degradation—Cables
- Cables and Concrete Aging and Degradation—Concrete
- Accident Tolerant Fuel Cladding
- General SCC and SCC Modelling
- BWR SCC and Water Chemistry
- Zirconium and Fuel Cladding
- Stainless Steel Aging and CASS
- Welds, Weld Metals, and Weld Assessments
- Plant Operating Experience
- IASCC Testing—Characterization
- IASCC Testing—Initiation and Growth
- PWR Oxides and Deposits
- PWR Secondary Side

This report has six sections.

The first section contains a general information and a summary of the conference.

The second section contains papers summaries (in general 2 to 3 pages).

The third section is the list of references.

The fourth section contains the nomenclature.

The fifth section is a list of acronyms.

The last section is a unit conversion table.

## 1.2 Summary

The use of Alloy 600 resulted in major maintenance costs for many plants worldwide. More and more components partially or totally made of Alloy 600 have been replaced with similar components where Alloy 600 has been replaced with Alloy 690. Given the disastrous field experience of Alloy 600, the industry wants to make sure that Alloy 690 will not in any way duplicate the bad Alloy 600 behaviour. Thus, any potential weakness of Alloy 690 is tracked by the researcher's community. Amongst these potential weaknesses are cold work and lead.

As concerns CW, it is essential to separate the effects of bulk CW from those of surface CW. There are several examples of surface CW in operating plants:

- CRDM and other nozzles with near surface cold worked layers from gun drilling or other forms of aggressive machining that are then deformed into an oval shape during welding to the upper head;
- SG divider plates with compressive layers induced by planning and/or grinding that are pulled into tension during the initial hydrotest;
- DMWs of Alloy 52/152 that are typically ground to prepare the surface of the weld for NDE.

There is a relatively small effect until a CW level of about 15%, and then the effect takes off, producing very striking effects at CW levels approaching 40%. Fortunately, the levels of CW that exist in nuclear components are limited by material specifications as well as ASME Boiler and Pressure Vessel Code requirements, to a bulk CW level of about 5%. The level of CW that exists in Alloy 52 and 152 weldments is about 10% in the HAZ adjacent to these welds.

Weld residual stresses and strains are the origins of most of the SCC in LWR structural materials.

For the ~30% Cr nickel alloys, clearly the concept of SCC immunity should be replaced with the concept of adequately low crack growth rate. The excellent resistance of Alloy 152 welds to PWSCC extends to aggressive BWR water chemistry conditions, with the same impact of CW.

Amongst all the mature PWSCC mitigation techniques available on the market, AREVA has selected the ultra-high-pressure cavitation peening. When replacement is not practical, PWSCC mitigation by the UHP CP technique is a cost-effective option to extend component life time. UHP CP is a mitigation technique which consists in projecting water at a pressure of 3,800 bars through a small diameter nozzle at high velocity towards a metal surface. As the water flow passes through the nozzle, the pressure drops below the saturated steam pressure, enabling the formation of cavitation bubbles. The cavitation cloud is sprayed at the surface to coat it with cavitation bubbles. These bubbles then collapse on the metal surface, causing localized shock waves which generate residual compressive stresses. These resulting compressive stresses eliminate the risk of PWSCC. However, the "big question" is: what about the evolution of these compressive stresses over the years given the operating loads, transients and events that can occur: high temperature, temperature variations, thermal cycling, pressure and pressure variations, start-up, shutdown. The process qualification tests along with supplemental tests performed by AREVA show that there is a limited decrease of the compressive stresses over the years.

Beginning of 2017, UHP CP has been implemented on three 4-loop PWR, RPV Heads at Byron 1 and 2 and Braidwood 1, with a 4th implementation in May, 2017. All four reactor heads have 78 Control Rod Drive Mechanisms type nozzles and 1 vent line. All RPV head UHP CP implementations have been completed within the 30-day total outage schedules.

Manufacturing techniques commonly used to fabricate metal components can induce residual stresses, plastic deformation and CW at the surface of components, whilst also affecting the surface

roughness. However, while chemical composition and heat treatment are usually tightly specified, specifications for machining on plant commonly only consider a required surface roughness. Results from some tests suggest that when a compressive residual stress is present at the surface, polishing to reduce the surface roughness removes that stress and reduces the nano-crystalline surface layer generated by machining, and is actually detrimental for PWSCC initiation resistance. This implies that surface residual stress, or the presence of a surface damaged layer, is a more dominate factor for PWSCC initiation than surface roughness.

Although Alloy 690 containing more than 7 wt% iron is not supposed to be susceptible to LRO, some laboratories still work on LRO issues, in the framework of life extension up to 60, 80 or even 100 years of operation. Upon thermal ageing, nickel–chromium alloys close to the stoichiometry of  $\text{Ni/Cr} = 2/1$  can undergo an ordering process; the ordered  $\text{Ni}_2\text{Cr}$  phase nucleates and grows, leading to a hardening of the alloy. Ordering occurs when the attractive force between different atoms is larger than that of same atoms. Based on the result from previous research on binary Ni–Cr alloys, the ordered phase can cause an increase in tensile strength, a decrease in ductility, and dimensional changes or internal stresses. Previous research results also show a hardening effect from ordering and a linear relationship between Vickers microhardness and yield strength. It is known that the fracture toughness decreases as yield strength increases, and fracture toughness is a key factor in stress corrosion cracking.

TEP measurements, which measure the electric potential when a temperature gradient is applied (Seebeck effect) are already performed in nuclear industry to follow spinodal decomposition of cast RCS elbows. It can also be applied to follow the ordering process of Ni–Cr systems. A good correlation between TEP and hardness is very often observed. Thus, TEP can be used as a LRO level indicator.

The trend of change in micro-hardness shows that the effect of hardening by LRO will reach saturation after 1000 h of heat treatment at 475°C, whereas the time to saturation for 418 and 373°C will be longer. By comparing the change in micro-hardness after ageing for 5000 h, the relationship between embrittlement and stoichiometry can be observed. As expected, the larger deviation from the  $\text{Ni/Cr} = 2$  stoichiometry leads to less embrittlement.

The effect of thermal aging on a material's properties is quite important; it can be linked to many problems. Many studies have investigated the effect of heat treatment on material properties. Although these valuable studies emphasized the influence of thermal aging on material properties, most involved SCC tests conducted on as-received materials that never experienced thermal aging, except short-term heat treatments, generally at high temperatures, above 600°C. However, significant differences may exist in the phases that form and in the relevant degradation mechanisms, as a consequence of low temperature thermal aging (e.g. at 320°C, the PWR operation temperature) versus high temperature heat treatment (above 600°C). Also, the studies generally use smooth-bar specimens tested under an uniaxial tensile stress state; however, most of cracked components experience a triaxial stress state. The reference [Yoo et al., 2017] shows that in SSRT tests using smooth specimens (uniaxial stress state), the material aged 10 years at 320°C shows the highest susceptibility to PWSCC, and the as-received condition shows the lowest susceptibility. This is attributed to the changes in morphology and number densities of precipitates. The semi-continuous precipitates and chromium depletion at grain boundaries make this material the most susceptible to PWSCC. On the other hand, the results of SSRT with notched specimens, which experience triaxial stress, are different from that of smooth specimens. In these tests, the material aged 20 years at 320°C has the highest susceptibility to PWSCC while the as-received condition has the lowest. The effect of triaxial stress state and associated shear stress may decrease due to change in precipitate morphology.

Generally inverse relationship between stress and time to failure exists, as would be expected. On a series of Alloy 718 specimens irradiated in the Halden Reactor under mechanical tensile stresses and in a chemical environment and temperature representative of PWR service conditions, no comparable relationship between stress and fluence at failure was observed, with fluences at failure ranging over four orders of magnitude and not correlated with stress. This suggests that for a given chemical environment (fixed, in this case), time is a better predictor of failure for a given stress than is fluence for fluences in this range, and neutron fluence is not a key experimental variable in these experiments. Failed specimens in this test lasted between 15 h and 10,890 h in-reactor, which may be compared with the 4.5 y (~40,000 h) design life of the component being modelled. Proprietary calculations show a

## 2 Papers summaries

### 2.1 PWR Nickel SCC – SCC

A great deal of PWSCC testing has been conducted on a range of A690 materials. The purpose of the paper [Bamford et al., 2017] is to discuss the basis for the effects of CW, and determine the levels of CW that exist in typical plant components. In this manner, the range of CW that should be included in the final recommended model and disposition curves for PWSCC of these materials can be determined.

In addressing this issue, it is essential to separate the effects of bulk CW from those of surface CW. There are several examples of surface CW in operating plants:

- CRDM and other nozzles with near surface cold worked layers from gun drilling or other forms of aggressive machining that are then deformed into an oval shape during welding to the upper head;
- SG divider plates with compressive layers induced by planning and/or grinding that are pulled into tension during the initial hydrotest;
- DMWs of Alloy 52/152 that are typically ground to prepare the surface of the weld for NDE.

Figure 2-1 left shows the nomenclature for CT specimen orientations with respect to a cylindrical forged product form, such as a CRDM nozzle. The orientation of an in-service crack propagating through-wall can be represented by the C-R or C-L orientations for an axial crack and by the L-R or L-C orientations for a circumferential crack. The R-L and R-C orientations are parallel to the pressurized surface, often termed the laminar direction; flaws in these orientations have never been observed in service. This is because there is little or no stress in the radial direction of a pressure vessel.

Figure 2-1 right shows the nomenclature for CT specimen orientations with respect to a plate or weld product form. The orientation of an in-service crack propagating through-wall can be represented by the T-S or T-L orientations for an axial crack and by L-S or L-T for a transverse crack. The S-L and S-T orientations correspond to the laminar direction, in which no cracks have been observed in service.

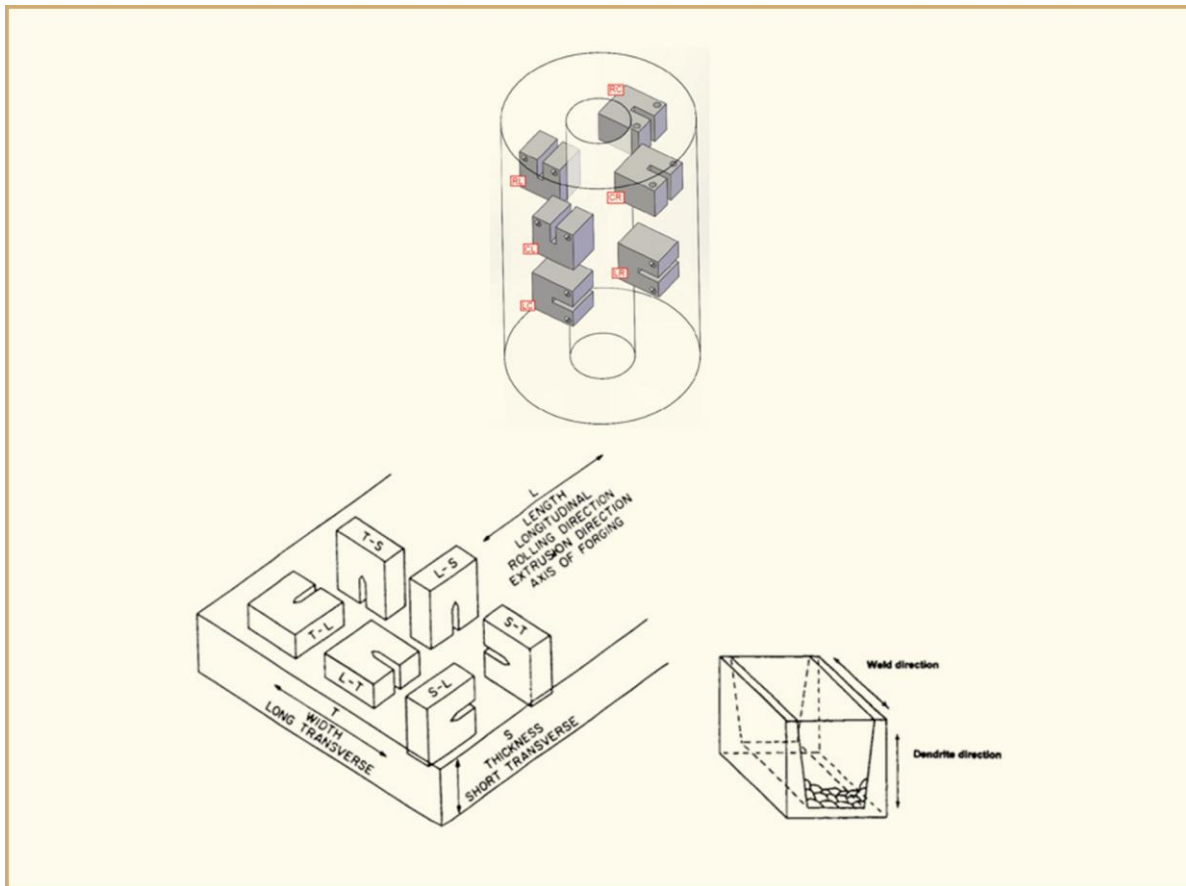


Figure 2-1: Left: specimen orientations for a cylindrical product form; right: specimen orientations for a plate or weld product form.

CW can significantly increase PWSCC rates in Alloy 690, for bulk cold work levels above about 15%. The Figure 2-2 shows that there is a relatively small effect until a CW level of about 15%, and then the effect takes off, producing very striking effects at CW levels approaching 40%. The levels of CW that exist in nuclear components are limited by material specifications as well as ASME Boiler and Pressure Vessel Code requirements, to a bulk CW level of about 5%. The level of CW that exists in Alloy 52 and 152 weldments is about 10% in the HAZ adjacent to these welds.

Crack growth disposition curves for Alloys 52, and 152 welds should be based on CGR tests conducted on weld specimens with no additional CW because these specimens retain the plastic strain produced during welding.



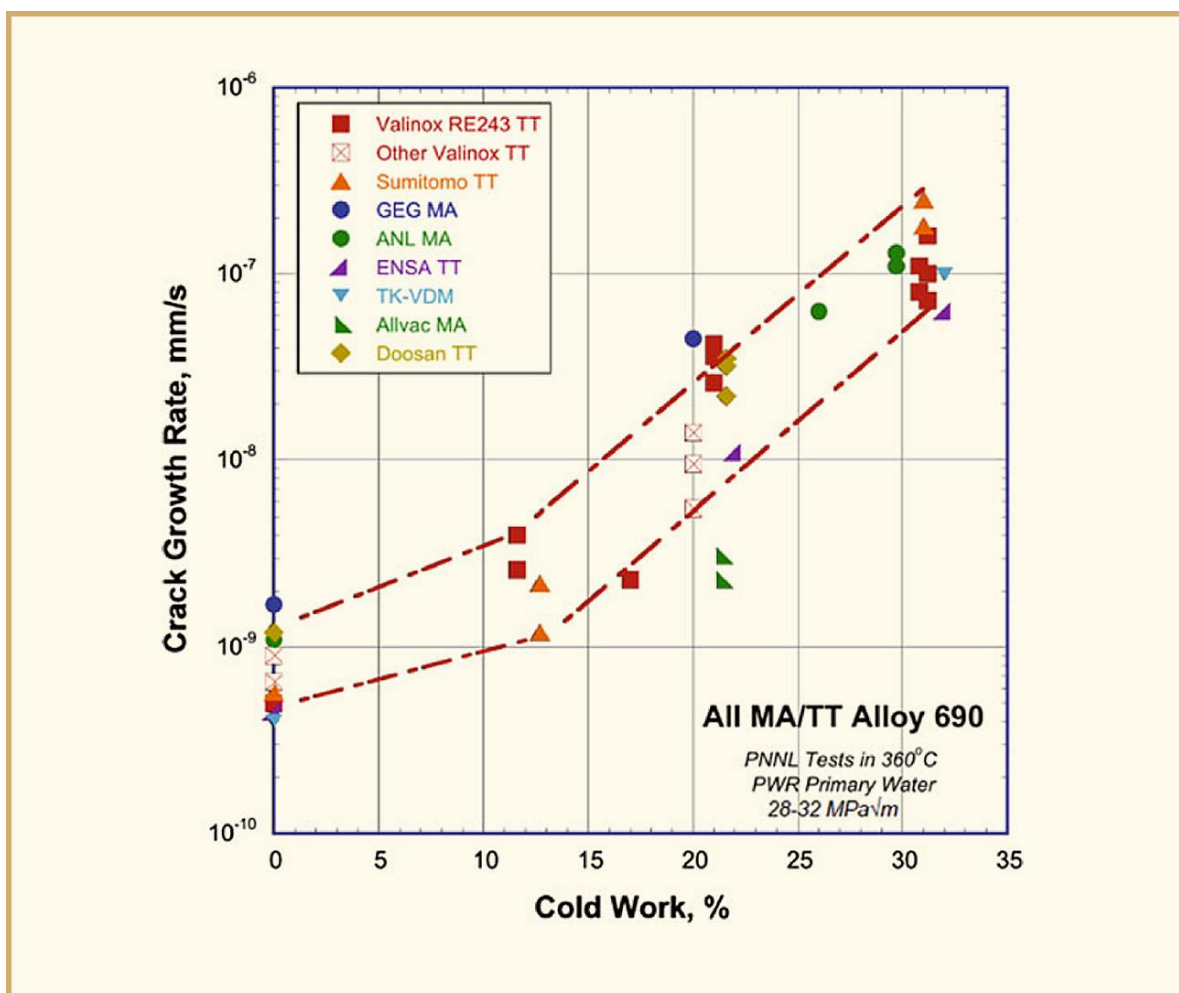


Figure 2-2: CW effects on measured SCC growth rates at  $K = 30\text{--}32 \text{ MPa}\sqrt{\text{m}}$ , for Alloy 690 Materials in the as-received MA or TT condition [Bamford et al., 2017].

SCC has been observed in many LWRs structural components, with the rate of SCC initiation and crack growth varying widely. Newer materials have been adopted in the last 2+ decades, primarily Alloy 690 and its weld metals, Alloys 52 & 152. Before careful testing was performed, these materials were widely viewed as immune to SCC, but it is now recognized that these materials exhibit at least some limited susceptibility to SCC. Because historical testing was often relatively simple and insensitive, combinations of materials, environments, and stressing conditions—such as unsensitized stainless steel and Alloy 690 in both PWR and BWR water—once generally viewed as immune to SCC have now been shown to be susceptible. The higher Cr content in Alloy 690 and its weld metals create greater challenges in melting and processing, and in welds, solidification causes partitioning of some elements to dendrite boundaries, and there is a greater propensity for various weld defects to occur.

Component lifetime is often viewed as being controlled by SCC initiation resistance, but there are dozens of materials and thousands of cases where the expected resistance to initiation was not realized. There is intrinsic optimism in the ASME Pressure Vessel and Boiler Codes, which simply mandate that SCC immunity exists, but typical 1–2-year evaluations in simple laboratory tests is not a strong basis for confidence in a 60+ year lifetime. To provide greater confidence in a 60–100 year lifetime, both SCC initiation and growth should be optimized, and indeed both are being pursued for Alloy 690 and its weld metals.

Weld residual stresses and strains are the origins of most of the SCC in LWR structural materials. In stainless steels, more of the weld residual strain develops in the HAZ than in Alloy 690 (Figure 2-3). These strains are accurately quantified using EBSD, which is a very high resolution and precise

technique for evaluating the misorientation that characterizes dislocation density from residual deformation.

Remarkably, the weld residual strains in Alloy 52/152 weld metal can be very high in isolated dendrites, exceeding 40% and even 50% in isolated dendrites.

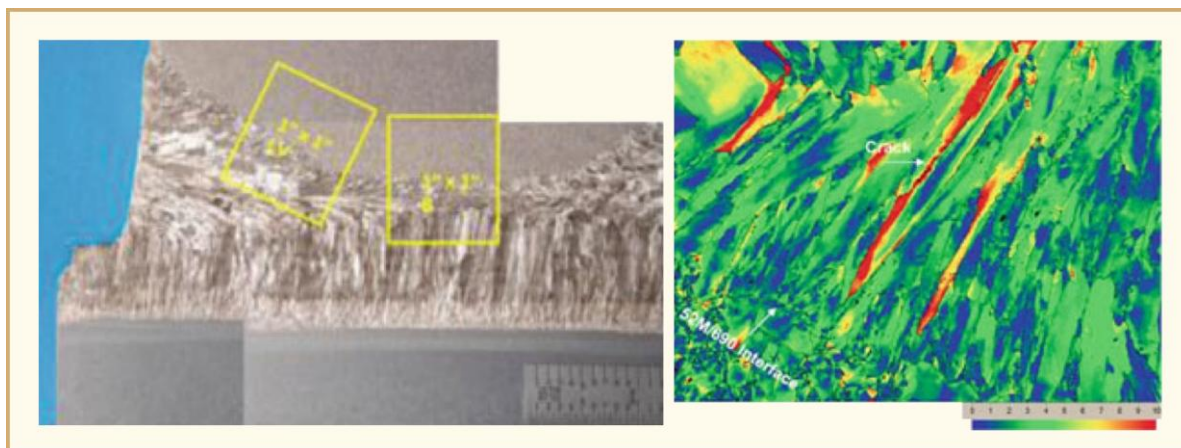


Figure 2-3: Left: characterization of a steam generator divider plate mock-up weld of Alloy 52M showing that the base metal had ~8% residual strain (from incomplete annealing), which increased to 12–14% in the base metal microstructure and 17–22% in the 690 composition (but different microstructure) of the partially melted zone. Right: EBSD strain map showing highly localized strains in isolated dendrites.

Into the partially melted zone and HAZ, the weld residual strains drop below ~20%. However, there has been little evaluation of the effect of welding defects on SCC. The reference [Andresen et al., 2017] reports the progress in an on-going research program on the SCC growth rate of Alloy 52, 152 and 52i weld metals.

For the ~30% Cr nickel alloys, there can be no question that some inherent susceptibility to SCC exists, and the SCC growth rate response of various heats, microstructures and types of CW of Alloy 690 were evaluated Alloy 690 in a related program. Clearly the concept of SCC immunity should be replaced with the concept of adequately low crack growth rate. The SCC resistance of 33 specimens of many Alloy 52/152/52i weld metals was evaluated over >315,000 h, including a number with weld defects and weld repairs, and their SCC growth rates were almost uniformly low.

These consistently low growth rates were observed in spite of many (reasonable) accelerants: moderate to high stress intensity factor (~30–45 MPa√m), high temperature (360°C) and dissolved H<sub>2</sub> values (26 cc/kg at 360°C) that are at the growth rate peak (at the Ni/NiO phase boundary). Additionally, very extensive and diverse approaches to IG transitioning were used over very long periods of time (over 171,000 h of total testing time), and multiple microstructures were examined in each weld (by advancing the crack by ~1 mm in fatigue and re-transitioning to condition that favours IGSCC).

All of the specimens tested at GE were fully engaged from the TG fatigue precrack. The extent of %IG ranged from small to medium (~50%), and did not appear to depend on the specific transitioning technique used. Higher %IG did not obviously translate to higher growth rates (within the context of the low growth rates at %IG observed), in part because TG crack advance was observed in most cases at constant K (no cycling). It should not be surprising that as alloys become highly resistant, the IG path becomes only slightly favoured over the TG path.

Good agreement on the crack growth rates of the high Cr weld metals—including on specific welds tested by multiple laboratories—was obtained. The only outliers related to Alloy 152 welds fabricated by ANL, and only when tested at ANL—other laboratories were unable to reproduce the higher growth rates despite extensive attempts (~50,000 h) on multiple specimens and multiple areas of each

weld microstructure. There is at time no explanation for the discrepancy, but in the broad spectrum of the international results, they are reasonably considered outliers at this time.

The excellent resistance—although not immunity—to SCC of these weld metals extends to aggressive BWR water chemistry conditions, although it's clear that the SCC resistance can be compromised by cold working the welds, which shouldn't occur in plant components.

Much of the focus of this study has been on weld defects, weld repairs and weld dilution zones, and only low growth rates have been observed. Regarding weld dilution zones, CGRs start decreasing significantly for Alloy 82 (as compared to Alloy 600), which is about 20% Cr and become very low when the Cr content exceeds 23% Cr (Figure 2-4). While some challenges remain in fabricating optimum high Cr welds, these data indicate that large defects can be tolerated because the SCC growth rates remain low.

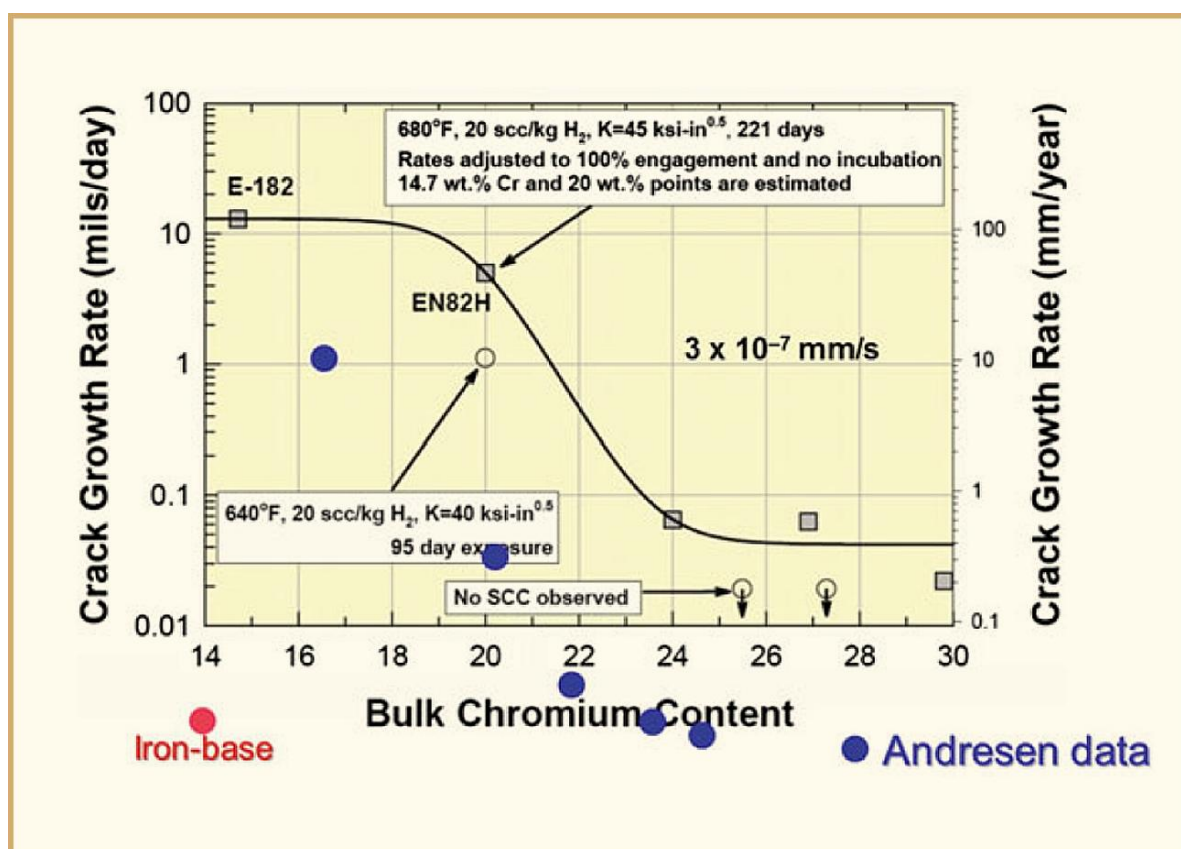


Figure 2-4: Summary of data on two-wire-feed welds that simulate weld dilution effects. Note that the 14% Cr point (in red) was a 50:50 mix of low alloy steel and a ~28% Cr nickel alloy, so the iron content is dramatically higher than in other welds [Andresen et al., 2017].

One of the formidable challenges facing corrosion engineers is developing tests to substantiate the high resistance of a material to environmental degradation issues definitively and efficiently. This is particularly difficult for materials with very long service lives such as the structural materials used in nuclear power plants. Generally, accelerated material degradation tests are designed and performed to generate data in relatively short timeframes (less than a year). The main accelerants that have been employed to enhance structural material SCC growth rate have been elevated temperature and material cold work. Composite material specimen testing provides an additional means to evaluate the SCC susceptibility of high SCC resistant materials.

The “composite arrest” test method, consists of fabricating composite material specimens consisting of a highly SCC susceptible material welded to a highly SCC resistant material. Specimens are configured such that SCC grows from the susceptible material toward the resistant material. Crack arrest within

the SCC resistant material provides confirmation that the material is extremely resistant to SCC in the test environment.

The chemical compositions of the materials used in the reference [Morton et al., 2017] test program are provided in Table 2-1. A listing of the SCC susceptible and resistant material pairs which were tested are shown in Table 2-2. 8N12/A600 and 8N12/EN82H specimens were “controls” intended to show that the cracking will not stop at the interface of two SCC susceptible materials. Composite arrest testing was performed with 0.6T compact tension specimens fabricated such that the air fatigue crack tip is in SCC susceptible material approximately 2.54 mm from the interface between the materials (Figure 2-5). Testing was performed at 360°C with 40 cc/kg of dissolved hydrogen. Specimens were removed from test after ~six months, 12 months and 18, 24 or 60 months to allow comparison of crack length at the different times and to assess if crack arrest occurred.

Table 2-1: Chemical composition (weight %) of the materials used in the composite arrest testing. 182 and 8N12 are equivalent materials which are highly susceptible to SCC growth [Morton et al., 2017].

Material	C	Ni	Cr	Fe	Ti	Nb/Ta	Mn	Mo
8N12 heat1	0.048	67.84	14.84	9.75	0.040	1.390	5.440	-
8N12 heat2	0.06	70.50	14.77	7.19	0.04	1.53	5.43	-
A600	0.07	75.77	15.04	7.87	0.35	-	0.22	-
A690	0.03	60.31	29.72	9.05	0.28	-	0.20	-
304 SS	0.041	8.60	18.30	Balance	-	-	1.73	0.04
EN625	0.01	64.6	21.9	0.6	0.25	3.55	0.00	5.8
A508	0.17	3.07	1.64	Balance	0.002	-	0.34	0.50
182	0.043	71.78	14.91	6.75	0.03	-	5.18	-
EN52 Sanicro	0.030	61.0	30.1	9.7	0.66	-	0.8	0.01
EN52 MSS	0.023	52.36	29.49	8.79	0.18	-	0.31	3.51
EN52i heat 1	0.040	63.88	26.98	2.55	0.37	-	3.04	0.003
EN52i heat 2	0.043	64.7	26.97	2.55	0.30	-	2.97	<0.01
EN82H	0.03	73.0	19.5	0.99	0.42	-	2.90	-
8N12H	0.07	68.1	15.0	6.7	0.72	-	6.5	-

© ANT International, 2018

Table 2-2: Material combinations used in the composite arrest testing [Morton et al., 2017].

Susceptible material	Resistant material	Designation in the tests
8N12 weld (heat 1)	Alloy 600	8N12/A690
8N12 weld (heat 1)	304 Stainless Steel	8N12/SS
8N12 weld (heat 1)	EN625 Hot Wire (HW)	8N12/EN625 HW <sup>a</sup>
8N12 weld (heat 1)	EN625 SMAW	8N12/EN625 SMAW <sup>b</sup>
8N12 weld (heat 2)	ASTM A508 Grade 4N	8N12/A508
182 weld	EN52 Sanicro 68HP	182/Sanicro
182 weld	EN52 MSS	182/MSS
182 weld	EN52i (heat 1)	182/EN52i-1
8N12H weld	EN52i (heat 2)	8N12 2H/EN52i-2
182 weld	EN82H	182/EN82H
182 weld	Alloy 600	182/A600

<sup>a</sup>: hot wire gas tungsten arc welding process  
<sup>b</sup>: shielded metal arc welding process

© ANT International, 2018

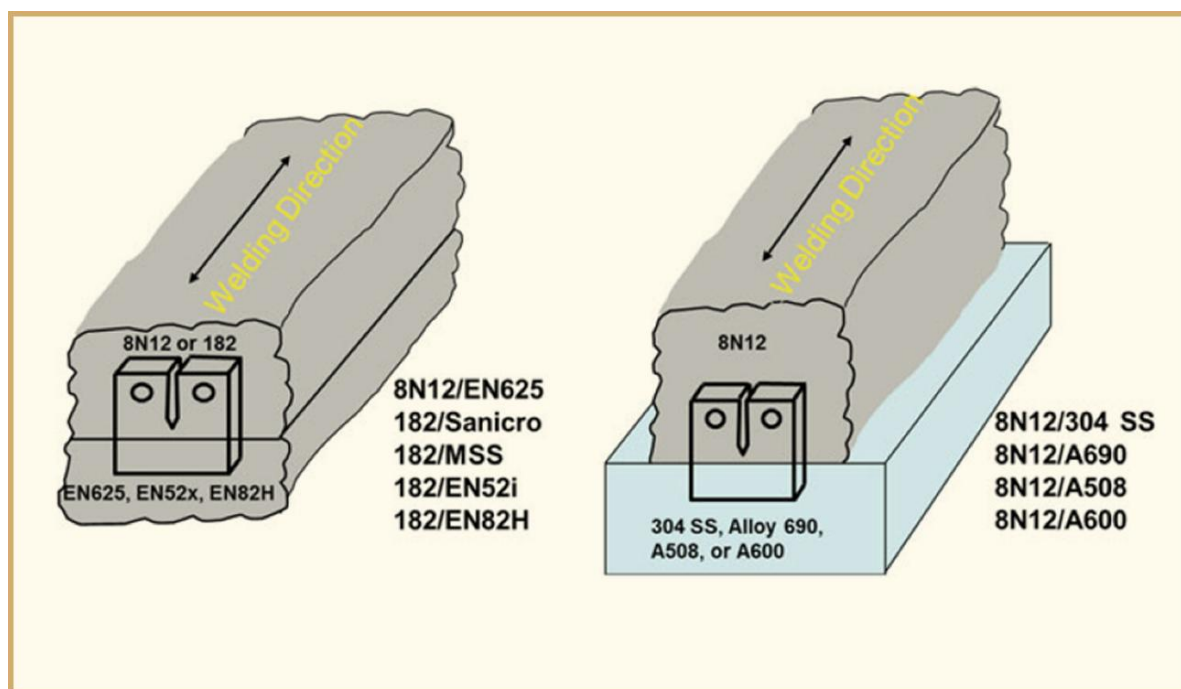


Figure 2-5: Schematic view of weld cradles used in the composite arrest test. 8N12 was welded atop of all materials [Morton et al., 2017].

These composite arrest specimen test results have confirmed that 304 SS, Alloy 690, A508, Alloy 625, and EN52 are all extremely resistant to SCC in primary water. Specifically, in aggressive composite arrest tests (360°C, high stress intensity factor), cracks growing within the SCC susceptible materials did not grow beyond the weld interfacial region into any of these SCC resistant materials except for the EN52 materials. The EN52 materials did grow beyond the interface in the first diluted bead, but at a significantly reduced rate and appeared to possibly arrest after a few months (Figure 2-6 and Figure 2-7).



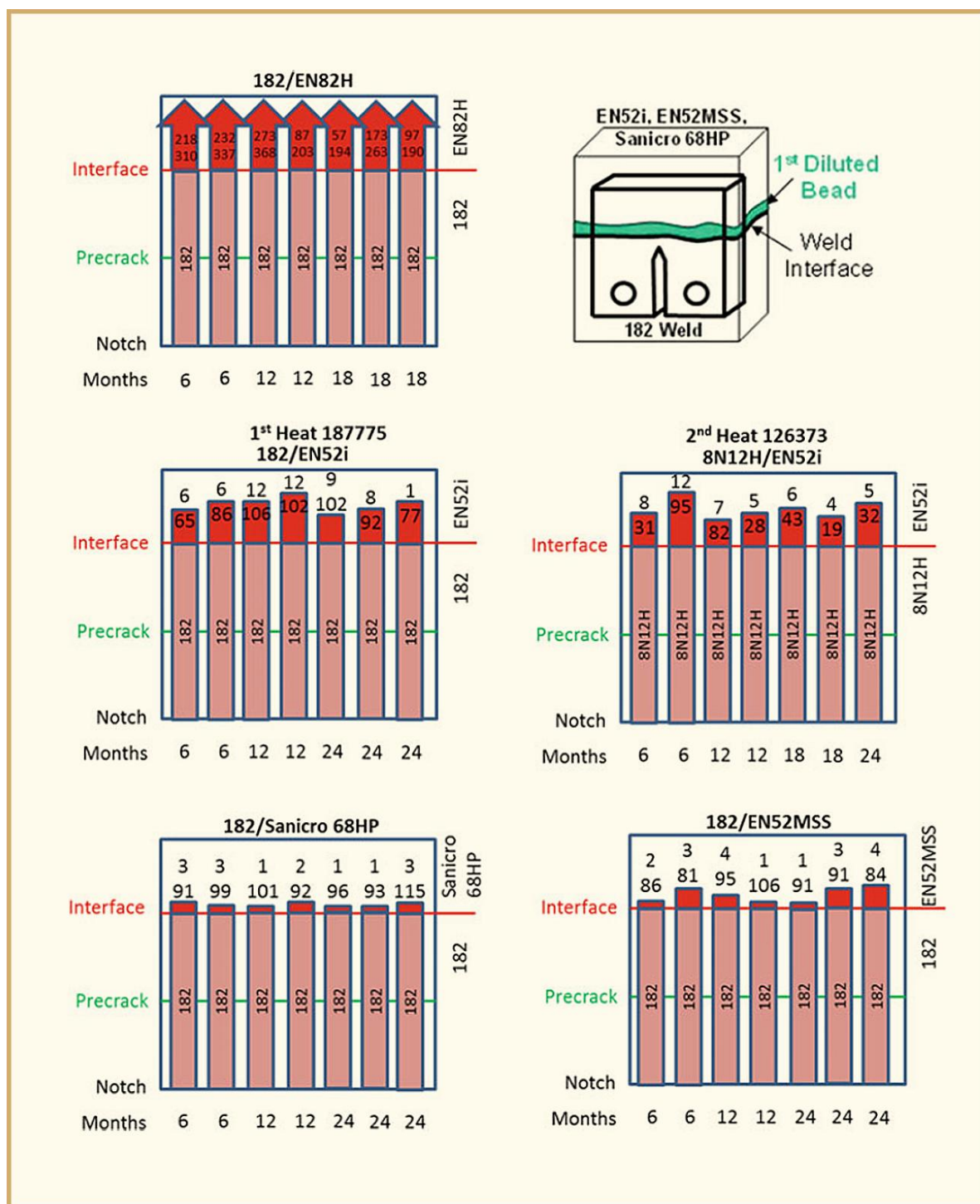


Figure 2-6: Composite arrest test result summary. Results show that the SCC readily advances in EN82H and grows slowly or arrests in EN52 variants (specimens are arranged by increasing test time, left-to-right, bar length is representative of the max extent of the SCC, the numbers above the bars represent the amount of average SCC growth in mils. The EN52 and EN82H specimens have a second smaller number that represents the average SCC beyond the interface) [Morton et al., 2017].



Figure 2-7: Fracture surface photographs for 182/EN52i specimens: results show a small amount of EN52i SCC extension which did not increase with additional test exposure. In contrast, significant EN82H SCC was observed after only 6 months. The scale mark is 0.1 in. (2.54 mm) [Morton et al., 2017].

The EN52i composite arrest specimens are representative of what a WOL dilution bead would look like in an EN52i overlay on Alloy 600, EN82H, or 182. Results with up to 2 years of exposure show less than 0.4 mm of average and 1.3 mm of maximum growth extent into the first diluted weld bead under aggressive test conditions. Although SCC growth was observed SCC growth likely arrested or possibly continued at an extremely slow rate in the aggressive high temperature (360°C) test environment.

Alloy 600 and EN82H composite material control specimens have shown that when two SCC susceptible materials are welded together SCC readily grows through and beyond the weld interface. These results were expected and confirm the underlying assumption from which the composite arrest program was developed, specifically that the presence of a weld/wrought or weld/weld interface in itself does not arrest SCC.

Results have shown that 8N12 weld metal enriched in iron due to SS dilution has relatively the same high SCC growth rate susceptibility as nominal 8N12 weld metal. In contrast, 8N12 weld metal enriched in chromium due to Alloy 690 or Alloy 625 dilution (~20 wt% compared to 15 wt% nominally in 8N12) is more resistant to SCC in primary water. These results support the view that elevated chromium level is the main reason why Alloy 690 (30% Cr), Alloy 625 (22% Cr), and EN52 (27–30% Cr) have vastly better SCC performance than Alloy 600 (15% Cr) (Figure 2-8). These results also suggest that iron concentration in itself is not the dominant parameter which accounts for SS's improved SCC performance relative to Alloy 600.

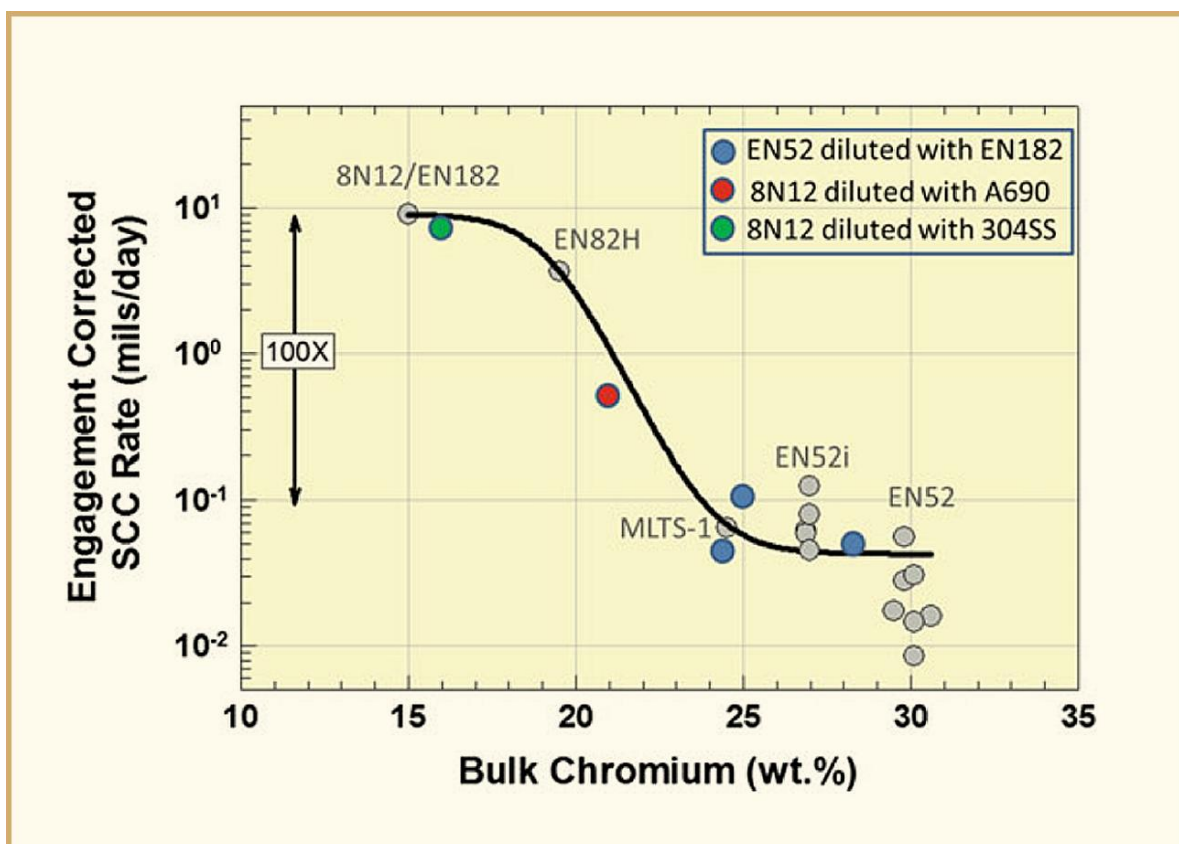


Figure 2-8: CGR of nickel alloy weld metals as a function of chromium level. Superimposed on this figure are CGRs observed in this study. Results illustrate a pronounced beneficial effect of increased chromium level [Morton et al., 2017].

Although a definitive statement cannot be made regarding SCC arrest versus very slow crack growth, 8N12/SS composite arrest specimens are speculated to have arrested SCC at the 8N12/SS interface and slow SCC growth is believed to have ensued in 8N12/A690, 8N12/A625 and 8N12/A508 specimens. This position is based upon analytical characterization results which showed no discernible microstructural or compositional difference between the regions in these composite arrest materials that underwent and did not undergo SCC.

The lack of SCC growth into the 304 SS HAZ in the composite arrest specimen testing was somewhat surprising since a level of ~12% equivalent plastic strain was measured in the HAZ. 304 SS SCC growth rates have been measured in deaerated water with equivalently cold worked levels of deformation (Figure 2-9). This disparity could be due to cold work deformation being different from welding induced deformation and/or the elevated 304 SS sulphur content (0.021%) mitigating the SCC in the composite arrest testing.



## References

- Ahn T.Y., Kim S.W., Hwang S.S., Kim H.P., *Relationship Among Dislocation Density, Local Strain Distribution, and PWSCC Susceptibility of Alloy 690*, Nuclear Materials Safety Research Division, Korea Atomic Energy Research Institute, Daejeon 34057, Republic of Korea, Proceedings of the 18th International Conference on Environmental Degradation of Materials in Nuclear Power Systems-Water Reactor, Portland USA, 2017.
- Ahonen M. et al., *Effect of Thermal Aging on Fracture Mechanical Properties and Crack Propagation Behavior of Alloy 52 Narrow-Gap Dissimilar Metal Weld*, (1) VTT Technical Research Centre of Finland Ltd., P.O. Box 1000, VTT, FI-02044 Espoo, Finland and Aalto University School of Engineering, P.O. Box 14200, FI-00760 Aalto, Finland, Proceedings of the 18th International Conference on Environmental Degradation of Materials in Nuclear Power Systems-Water Reactor, Portland USA, 2017.
- Andresen P., Morra M. and Ahluwalia K., *SCC of Alloy 152/52 Welds Defects, Repairs and Dilution Zones in PWR Water*, (1) Andresen Cons., 12204 Wildwood Park Pl, Bakersfield, CA 93311, USA, (2) GE Research, One Research Circle CE 2545, Schenectady, NY 12309, USA, (3) EPRI, 3420 Hillview Ave, Palo Alto, CA 94304, USA, Proceedings of the 18th International Conference on Environmental Degradation of Materials in Nuclear Power Systems-Water Reactor, Portland USA, 2017.
- Aoki S., Kondo K., Kaji Y., Yamamoto M., *Effect of Long-Term Thermal Aging on SCC Initiation Susceptibility in Low Carbon Austenitic Stainless Steels*, Japan Atomic Energy Agency, Nuclear Science and Engineering Center, 2-4 Shirakata, Tokai-Mura, Naka-Gun, Ibaraki 319-1195, Japan, Proceedings of the 18th International Conference on Environmental Degradation of Materials in Nuclear Power Systems-Water Reactor, Portland USA, 2017.
- Arioka K. et al., *Degradation of Alloy 690 After Relatively Short Times*. Corrosion 72, 1252-1268, Houston, 2016.
- Arioka K. et al., *Effect of Ni and Cr on IGSCC Growth Rate of Ni-Cr-Fe Alloys in PWR Primary Water*, in Proceedings of the International Symposium FONTEVRAUD 8, Avignon, CD-Rom. France, 15-18 Sept, 2014.
- Arioka K., Yamada T., Miyamoto T., Terachi T., *SCC Initiation of CW Alloy TT690 and Alloy 600 in PWR water*, (1) Institute of Nuclear Safety Systems, Inc., Japan, (2) Kobe Material Testing Laboratory Co., Ltd, Japan, Proceedings of the 17th International Conference on Environmental Degradation of Materials in Nuclear Power Systems-Water Reactor, Ottawa, Canada, 2015.
- Bamford W., Fyfe S., Pathania R., Crooker P., *Applicability of Alloy 690/52/152 Crack Growth Testing Conditions to Plant Components*, (1) Westinghouse, Pittsburgh, PA, USA, (2) AREVA Inc., Lynchburg, VA, USA, (3) EPRI, Palo Alto, CA, USA, Proceedings of the 18th International Conference on Environmental Degradation of Materials in Nuclear Power Systems-Water Reactor, Portland USA, 2017.
- Bertali G., Scenini F. and Burke M.G., *Advanced Microstructural Characterization of the Intergranular Oxidation of Alloy 600*. Corros. Sci. 100, 474-483, 2015.
- Bertali G., Scenini F. and Burke M.G., *The Effect of Residual Stress on Preferential Intergranular Oxidation of Alloy 600*. Corros. Sci. 101, 494-507, 2016.
- Bertali G., Scenini F. and Burke M.G., *The Intergranular Oxidation Susceptibility of Thermally-Treated Alloy*. Corros. Sci. 114, 112-122, 2017.
- Bjurman M. et al., *Root Cause Analysis of Cracking in Alloy 182 BWR Core Shroud Support Leg Cracks*, (1) Studsvik Nuclear AB, Nyköping, Sweden, (2) Idaho National Laboratory, Idaho Falls, USA and (3) Forsmark Kraftgrupp AB, Forsmark, Sweden, Proceedings of the 18th International Conference on Environmental Degradation of Materials in Nuclear Power Systems-Water Reactor, Portland USA, 2017.

- Holdsworth S. et al., *Investigations of the Dual Benefits of Zinc Injection on Cobalt-60 Uptake and Oxide Film Formation Under Boiling Water Reactor Conditions*, University of Manchester, Manchester, UK, Proceedings of the 18th International Conference on Environmental Degradation of Materials in Nuclear Power Systems-Water Reactor, Portland USA, 2017.
- Hosemann P. et al., in *Proceeding of the 18<sup>th</sup> International Conference on Environmental Degradation of Materials in Nuclear Power Systems*, 2016.
- Huin N., Calonne O., Herbst M., Kilian R., *SCC of Austenitic Stainless Steels Under Off-Normal Water Chemistry and Surface Conditions - Part I: Surface Conditions and Baseline Tests in Nominal PWR Primary Environment*, (1) AREVA NP Technical Center, 30 Boulevard de L'Industrie—Espace Magenta—BP 181, 71205 Le Creusot Cedex, France and (2) AREVA GmbH Technical Center, Paul-Gossen-Str. 100, 91052 Erlangen, Germany, Proceedings of the 18th International Conference on Environmental Degradation of Materials in Nuclear Power Systems-Water Reactor, Portland USA, 2017.
- Hyres J., Thompson R. and Batton J., *Laboratory Analysis of a Leaking Letdown Cooler from Oconee Unit 3*, (1) BWX Technologies, Inc., 2016 Mt. Athos Road, Lynchburg, VA 24504-5447, USA, (2) Duke Energy, 526 South Church Street, Charlotte, NC 28202, USA and (3) Duke Energy, Oconee Nuclear Station, Seneca, SC 29672, USA, Proceedings of the 18th International Conference on Environmental Degradation of Materials in Nuclear Power Systems-Water Reactor, Portland USA, 2017.
- Ishizaki T. et al., *Development of High Irradiation Resistant and Corrosion Resistant Oxide Dispersion Strengthened Austenitic Stainless Steels*, (1) Research & Development Group, Hitachi Ltd., 1-1 Omika-cho 7-chome, 317-8511 Hitachi-shi, Ibaraki-ken, Japan and (2) Kyoto University, Institute of Advanced Energy, Gokasho, 611-0011 Uji-shi, Kyoto-fu, Japan, Proceedings of the 18th International Conference on Environmental Degradation of Materials in Nuclear Power Systems-Water Reactor, Portland USA, 2017.
- Jiao Z., Was G., Miura T., Fukuya K., *Aspects of Ion Irradiations to Study Localized Deformation in Austenitic Stainless Steels*. J. Nucl. Mater. 452, 328-334, 2014.
- Kai J. et al., *The Effects of Heat Treatment on the Chromium Depletion, Precipitate Evolution, and Corrosion Resistance of Inconel Alloy 690*. Metall. Trans. A 20, 2057-2067, 1989.
- Kako K., Miyahara Y., Arai T., Mayuzumi M., *Effects of Chemical Compositions and Grain Size on Stress Corrosion Cracking of Austenitic Stainless Steel in High Temperature Water*, (CRIEPI Report, Q07020), 2008.
- Killian R., in *Workshop on Detection, Avoidance, Mechanism, Modeling and Prediction of SCC Initiation in Water-Cooled Nuclear Reactor Plants*, Beaune France, 7-12 Sept, 2008.
- Kim S. and Kim Y.S., *Effects of Ordering Reaction on Mechanical Behavior in Alloy 690*, Nuclear Materials Development, Presentation at Aalto University, 2013.
- Kopcash J., Varela J., Huie H., Depta G., *Confirmation of On-Line NobleChem™ (OLNC) Mitigation Effectiveness in Operating Boiling Water Reactors (BWRs)*, GE-Hitachi Nuclear Energy LLC and EPRI, Wilmington, USA, Proceedings of the 18th International Conference on Environmental Degradation of Materials in Nuclear Power Systems-Water Reactor, Portland USA, 2017.
- Koshiishi M. and Shigenaka N., *Formation of He Bubbles by Repair-Welding in Neutron-Irradiated Stainless Steels Containing Surface Cold-Worked Layer*, (1) Nippon Nuclear Fuel Development Co., Ltd, 2163 Narita-Cho, Oarai-Machi, Higashi-Ibaraki-Gun, Ibaraki-Ken 311-1313, Japan and (2) Hitachi-GE Nuclear Energy, Ltd, 1-1, Saiwai-cho 3-chome, Hitachi-Shi, Ibaraki-Ken 317-0073, Japan, Proceedings of the 18th International Conference on Environmental Degradation of Materials in Nuclear Power Systems-Water Reactor, Portland USA, 2017.

- Meric de Bellefon G., van Duysen J.C. and Sridharan K., *In Situ and Ex Situ Observations of the Influence of Twin Boundaries on Heavy Ion Irradiation Damage Effects in 316L Austenitic Stainless Steels*, (1) Department of Nuclear Engineering, University of Wisconsin, Madison, USA, (2) Unité Matériaux et Transformation (UMET), CNRS, Université de Lille 1, Villeneuve-d'Ascq, France, Department of Nuclear Engineering, University of Tennessee, Knoxville, USA and EDF—Centre de Recherche des Renardieres, Moret sur Loing, France, Proceedings of the 18th International Conference on Environmental Degradation of Materials in Nuclear Power Systems-Water Reactor, Portland USA, 2017.
- Michalička J., Jiao Z. and Was G., *Radiation-Induced Precipitates in a Self-ion Irradiated Cold-Worked 316 Austenitic Stainless Steel Used for PWR Baffle-Bolts*, (1) CEITEC Nano Research Infrastructure, Brno University of Technology, Purkynova 123, 61200 Brno, Czech Republic, (2) Department of Nuclear Engineering and Radiological Sciences, University of Michigan, 1921 Cooley Bld, Ann Arbor, MI 48109, USA, Proceedings of the 18th International Conference on Environmental Degradation of Materials in Nuclear Power Systems-Water Reactor, Portland USA, 2017.
- Miura T. et al., *A study for Effects of Grain Size on Occurrence of IASCC Effects of Grain Size on Localized Deformation of Irradiated Stainless Steel*. J. Inst. Nucl. Saf. Syst. 18, 211-217, 2011.
- Miura Y., Miyahara Y., Kako K., Sato M., *Effects of Plastic Strain and Stress Distribution on SCC Initiation in High Temperature Water*, in CORROSION 2013, NACE International, 2013.
- Morton D. et al., *Stress Corrosion Crack Growth Rate Testing of Composite Material Specimens*, Knolls Atomic Power Laboratory Bechtel Marine Propulsion Corporation, P.O. Box 1072, Schenectady, NY 12301-1072, USA, Proceedings of the 18th International Conference on Environmental Degradation of Materials in Nuclear Power Systems-Water Reactor, Portland USA, 2017.
- Moss T. and Was G.S., *Accelerated Stress Corrosion Crack Initiation of Alloys 600 and 690 in Hydrogenated Supercritical Water*. Met. Mat. Trans. 48A, 1613-1628, 2017.
- Moss T.E., Brown C.M. and Young G.A., *The Effect of Hardening via Long Range Order on the SCC and LTCP Susceptibility of a Nickel-30 Chromium Binary Alloy*, (1) Naval Nuclear Laboratory, Bechtel Marine Propulsion Corporation, Niskayuna, NY 12309, USA, (2) Naval Nuclear Laboratory, Bechtel Marine Propulsion Corporation, West Mifflin, PA 15122, USA and (3) Dominion Engineering Inc., Reston, VA 20191, USA, Proceedings of the 18th International Conference on Environmental Degradation of Materials in Nuclear Power Systems-Water Reactor, Portland USA, 2017.
- Mouginot R. et al., *Development of Short-Range Order and Intergranular Carbide Precipitation in Alloy 690 TT upon Thermal Ageing*, (1) Department of Mechanical Engineering, Aalto University School of Engineering, Otakaari 4, 02150 Espoo, Finland, (2) Department of Chemistry, University of Helsinki, A.I. Virtasen aukio 1, P.O. Box 55, 00014 Helsinki, Finland, (3) VTT Technical Research Centre of Finland Ltd., Kivimiehentie 3, 02150 Espoo, Finland, Proceedings of the 18th International Conference on Environmental Degradation of Materials in Nuclear Power Systems-Water Reactor, Portland USA, 2017.
- Murayama M. et al., *The Combined Effect of Molybdenum and Nitrogen on the Fatigued Microstructure of 316 Type Austenitic Stainless Steel*, Scripta Mater. 41, 467-473, 1999.
- Nguejio J. et al., *Diffusion Processes as Possible Mechanisms for Cr Depletion at SCC Crack Tip*, (1) MINES ParisTech, PSL Research University, MAT-Centre des matériaux, CNRS UMR 7633, BP 87 91003 Evry, France, (2) DEN-Service de la Corrosion et du Comportement des Matériaux dans leur Environnement (SCCME), CEA, Université Paris-Saclay, 91191 Gif-sur-Yvette, France, (3) Laboratoire GEMaC, UMR 8635, CNRS—Université de Versailles, 45 Avenue des Etats-Unis, 78035 Versailles Cedex, France, Proceedings of the 18th International Conference on Environmental Degradation of Materials in Nuclear Power Systems-Water Reactor, Portland USA, 2017.

## Nomenclature

µm	micro meter
appm	part per million in atoms
at. %	atomic percentage
C-L	Circumferential – Longitudinal
C-R	Circumferential – Radial
D <sub>2</sub> O	Heavy Water
DBTT	Ductile-Brittle Transition Temperature
dpa	displacement per atom
fcc	face centred cubic
K	Stress intensity factor
L-C	Longitudinal - Circumferential
L-R	Longitudinal – Radial
L-S	Longitudinal – Short transverse
L-T	Longitudinal – long Transverse
meV	Mega electron Volt
mm/s	millimetres per second
mN	milliNewton
MPa	MegaPascal
nm	nano meter
ppm	part per million
R-C	Radial – Circumferential
R-L	Radial – Longitudinal
S-L	Short transverse - Longitudinal
S-T	Short transverse – long Transverse
T	Tritium
TE	Total Elongation
T-L	long Transverse - Longitudinal
T-S	long Transverse – Short transverse
USE	Upper Shelf Energy
wt%	Percentage in weight
YS	Yield Stress

## List of Abbreviations

ABWR	Advanced Boiling Water Reactor
ANL	Argonne National Laboratory
ANO	Arkansas Nuclear One
APT	Atom Probe Tomography
ASME	American Society of Mechanical Engineers
ASTM	American Society for Testing and Materials
ATEM	Analytical Transmission Electron Microscopy
B&W	Babcock and Wilcox
BCC	Body-Centered Cubic
BDBA	Beyond Design Basis Accident
BF	Bright Field
BFB	Baffle Former Bolt
BHDL	Bottom Head Drain Line
BMI	Bottom Mounted Instrumentation
BMN	Bottom Mounted Nozzles
BSE	Back Scattered Electrons
BWR	Boiling Water Reactor
BWRVIP	Boiling Water Reactor Vessel and Internals Program
CASS	Cast Austenitic Stainless Steels
CBB	Crevice Bent Beam
CDZ	Carbon-Depleted Zone,
CERT	Constant Extension Rate Test
CF	Corrosion Fatigue
CGR	Crack Growth Rate
CNL	Canadian Nuclear Laboratories
CP	Cavitation Peening or Chemical Polishing
CRDM	Control Rod Drive Mechanism
CT	Compact Tension
CTE	Coefficient of Thermal Expansion
CVCS	Chemistry and Volume Control System
CW	Cold Work
DA	Direct Aged
DAP	Dimensional Atom Probe
DCPD	Direct Current Potential Drop
DF	Dark Field
DH	Dissolved Hydrogen
DH <sub>2</sub>	Dissolved Hydrogen
DIC	Differential Interference Contrast
DIGM	Diffusion-Induced Grain boundary Migration
DLs	Disposition Lines
DMW	Dissimilar Metal Weld
DO	Dissolved Oxygen
EAC	Environmentally Assisted Cracking/Corrosion
EBSD	Electron BackScattered Diffraction
ECP	Electrochemical Corrosion Potential
EDM	Electro Discharge Machining
EDS	Energy Dispersive Spectroscopy
EDX	Energy Dispersive X-ray
EELS	Electron Energy Loss Spectrometry
EFTEM	Energy-Filtering Transmission Electron Microscopy
ENSI	Swiss Federal Nuclear Safety Inspectorate
EOC	End-Of-Cycle
EPD	Electrical Potential Drop
EPRI	Electric Power Research Institute
ET	Eddy current Testing

## Unit conversion

TEMPERATURE		
$^{\circ}\text{C} + 273.15 = \text{K}$	$^{\circ}\text{C} \times 1.8 + 32 = ^{\circ}\text{F}$	
T(K)	T( $^{\circ}\text{C}$ )	T( $^{\circ}\text{F}$ )
273	0	32
289	16	61
298	25	77
373	100	212
473	200	392
573	300	572
633	360	680
673	400	752
773	500	932
783	510	950
793	520	968
823	550	1022
833	560	1040
873	600	1112
878	605	1121
893	620	1148
923	650	1202
973	700	1292
1023	750	1382
1053	780	1436
1073	800	1472
1136	863	1585
1143	870	1598
1173	900	1652
1273	1000	1832
1343	1070	1958
1478	1204	2200

Radioactivity	
1 Sv	= 100 Rem
1 Ci	= $3.7 \times 10^{10}$ Bq = 37 GBq
1 Bq	= $1 \text{ s}^{-1}$

MASS	
kg	lbs
0.454	1
1	2.20

DISTANCE	
x ( $\mu\text{m}$ )	x (mils)
0.6	0.02
1	0.04
5	0.20
10	0.39
20	0.79
25	0.98
25.4	1.00
100	3.94

PRESSURE		
bar	MPa	psi
1	0.1	14
10	1	142
70	7	995
70.4	7.04	1000
100	10	1421
130	13	1847
155	15.5	2203
704	70.4	10000
1000	100	14211

STRESS INTENSITY FACTOR	
MPa $\sqrt{\text{m}}$	ksi $\sqrt{\text{inch}}$
0.91	1
1	1.10